

Ultrasonic Spectrometry of Triethylenediamine Aqueous Solutions. Protolysis and Supramolecular Structures

A. Rupprecht and U. Kaatze*

Drittes Physikalisches Institut, Georg-August-Universität, Bürgerstrasse 42-44, D-37073 Göttingen, Germany

Received: July 30, 1997; In Final Form: October 6, 1997[⊗]

At 25 °C the ultrasonic absorption coefficient of aqueous solutions of triethylenediamine (TED) has been measured as a function of frequency ν (200 kHz $\leq \nu \leq$ 4.6 GHz) and solute concentration c (0.0025 mol/L $\leq c \leq$ 2.56 mol/L). One solution has also been studied at 15 °C and 35 °C. To look for the dependence upon the pH some spectra have been recorded with NaOH or HCl added. The measured spectra have been analyzed in terms of a model relaxation function containing a Debye relaxation term and a term that represents noncritical fluctuations in the concentration. The Debye term is related to the protolysis of the TED molecule. Depending on the pH either the first or the second step of protonization of TED is reflected by the relaxation process. The forward and reverse reaction rates and the isentropic reaction volume have been determined from the relaxation parameters and it has been found that the amplitude and relaxation time of the Debye term can be described by one set of activity coefficients for the first protolysis reaction. The noncritical concentration fluctuations are analytically represented by an extended version of the Romanov–Solov'ev theory that also considers spatial correlations. At $c > 0.5$ mol/L a correlation length of about 4 Å is found. The finding of TED association at an elevated solute content is consistent with previous results from dielectric spectrometry.

1. Introduction

The delicate balance between hydrogen interactions and hydrophobic effects is of considerable significance in determining the structure and microdynamics of aqueous solutions of a variety of solutes, including biomolecules.^{1–7} It has been shown recently that, also depending on steric properties of the solute, aqueous solutions tend to form rapidly fluctuating mesoscopic structures as the number of hydrophobic groups per solute molecules increases.^{8–12} Among the series of binary aqueous systems that have been extensively studied so far, mixtures of water with monohydric alcohols,⁸ ethylene glycol ethers,¹² carboxylic acids,^{10,12} and tetraalkylammonium salts¹¹ exhibit tendencies toward a microheterogeneous structure.

Triethylenediamine exhibits outstanding solvation characteristics in aqueous solutions.^{13–16} The hydration properties suggest that this molecule induces an almost optimum clathrate-type water structure around itself. Obviously, at low and moderate solute concentration, the molecular size and globular shape of triethylenediamine, its low flexibility, and also the position of its nitrogen lone electron pairs relative to the position of the inert ethylene groups contribute to the formation of a particular stable shell of hydration water. The question arises whether such a solute is also capable of forming supramolecular structures of low water content or whether triethylenediamine monomers in a solution are stabilized by their hydration water clathrates. On one hand, *n*-alkyl groups, which are especially effective in promoting “hydrophobically bound” aggregates such as micelles, are missing. In addition, the nearly perfect spherical shape of the molecule is expected to prevent the molecule from stacking mechanisms characteristic of various cyclic bases such as purines.¹⁷ On the other hand, however, the solubility of triethylenediamine in water is rather high (about 3 mol/L, 25 °C), thus suggesting the presence of association effects.

To look for the existence/nonexistence of hydrophobic association mechanisms in aqueous solutions of triethylenedi-

amine we performed a systematic ultrasonic relaxation study as a function of the solute concentration. Coupling to fluctuations in the concentration, sonic fields have turned out to be particularly sensitive in indicating a microheterogeneous liquid structure.^{8–12} Since protolysis of the cyclic base is also expected to contribute to the acoustic spectra of the solutions, measurements have been conducted over an as broad as possible frequency range (200 kHz $\leq \nu \leq$ 4.6 GHz) in order to enable a clear separation of the different relaxation mechanisms from the spectra. Some solutions have been studied with hydrogen chloride or sodium hydroxide added to look for the dependence upon the pH. Most measurements have been performed at 25 °C. To be able to estimate the free activation energy of the protolysis reaction one solution has been measured at 15 and 35 °C.

2. Experimental Section

Aqueous Solutions. Triethylenediamine (TED, 1,4-diazabicyclo[2,2,2]octane, N(CH₂CH₂)₃N, >98%), HCl (Titrisol), and NaOH (Titrisol) have been used as delivered by the manufacturer (Merck, Darmstadt, Germany). Water was bidistilled and additionally deionized by mixed-bed ion exchange. The TED concentration of the solutions has been adjusted by weighing appropriate amounts of the substance into suitable flasks that were filled up to the line measure with water or with the HCl or NaOH solution, respectively. The density of the TED solutions has been measured pycnometrically. The (static) shear viscosity η_s of the sample liquids has been determined by using a falling ball viscometer (Haake, Model B/BH). A survey of the solutions is given in Table 1.

Ultrasonic Absorption Spectrometry. Acoustical absorption spectra of liquids are usually described by two terms¹⁸

$$\alpha(\nu) = B'\nu^2 + \alpha_{\text{exc}}(\nu) \quad (1)$$

where $B' = (B/c_s)$ represents the frequency independent part in the total absorption coefficient α and α_{exc} denotes the excess

[⊗] Abstract published in *Advance ACS Abstracts*, November 15, 1997.

TABLE 1: Molar Concentration c , Molality m , Mass Fraction y , and Mole Fraction x of the Solute as Well as Density ρ , Shear Viscosity η_s , and Sound Velocity c_s at around 1 MHz of the Solutions for Aqueous TED Systems

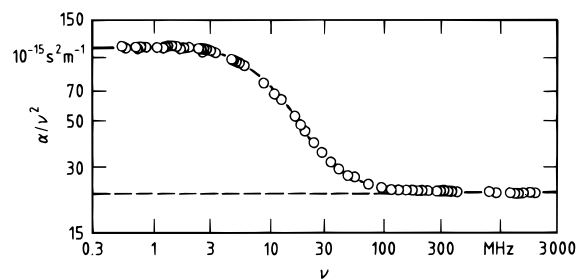
c , mol/L $\pm 0.2\%$	m , mol/kg $\pm 0.1\%$	y , 10^{-2} $\pm 0.1\%$	x , 10^{-2} $\pm 0.2\%$	ρ , g/cm ³ $\pm 0.1\%$	η_s , 10^{-3} Pa s $\pm 0.2\%$	c_s , m/s $\pm 0.1\%$
25 °C, Water, pH = 10.0–11.5						
0.0025	0.0025	0.028	0.0045	0.9970	0.896	1497.0
0.010	0.0100	0.112	0.0180	0.9967	0.898	1496.6
0.040	0.0402	0.449	0.0724	0.9969	0.899	1500.3
0.250	0.257	2.80	0.461	0.9985	1.03	1514.6
0.601	0.643	6.73	1.15	1.001	1.22	1542.1
0.904	1.00	10.1	1.77	1.004	1.43	1566.9
1.52	1.80	16.8	3.15	1.011	2.00	1618.3
2.04	2.58	22.4	4.44	1.018	2.76	1661.6
2.56	3.47	28.0	5.89	1.025	4.00	1710.1
15 °C, Water						
0.010	0.0100	0.112	0.0180	0.9986	1.15	1467.8
35 °C, Water						
0.010	0.0100	0.112	0.0180	0.9939	0.728	1520.8
25 °C, 0.01 mol/L NaOH, pH = 12.0						
0.040	0.0402	0.449	0.0724	0.9974	0.902	1500.5
25 °C, 0.1 mol/L NaOH, pH = 13.0						
0.908	1.00	10.1	1.77	1.009	1.43	1576.6
25 °C, 0.08 mol/L HCl, pH = 2.2						
0.04	0.0403	0.450	0.0725	0.9988	0.889	1501.9

TABLE 2: Relative Error in the Ultrasonic Absorption Coefficient α

ν , MHz	0.2–1	1–8	8–10	10–30	30–500	500–4600
$\Delta\alpha/\alpha$	0.07	0.05	0.06	0.02	0.008	0.015

contributions that may be due to chemical relaxations,¹⁹ concentration fluctuations^{11,12,20,21} as well as dissipation mechanisms related to scattering.²² Here, ν denotes the frequency and c_s the sound velocity of the liquid. Within the frequency range under consideration ($0.2 \text{ MHz} \leq \nu \leq 4600 \text{ MHz}$) the absorption coefficient changes by more than a factor of 10^9 . To cover this large range of α values and the broad range of different wavelengths, two different methods of measurement and a total of seven different cells have been used. Each sample cell was matched to a particular frequency range. By use of a planoconcave²³ ($0.2 \leq \nu \leq 2.8 \text{ MHz}$) and a biplanar²⁴ ($1 \leq \nu \leq 15 \text{ MHz}$) cavity resonator, quality factor measurements have been performed in the lower frequency range. To properly account for higher-order modes within the cavity resonator we always measured the complete transfer function around a main resonance peak of interest and derived the desired resonance frequency and quality factor from a multipoint fit of the scan to suitable theoretical expressions. Reference measurements have been performed with liquids of carefully adjusted sound velocity and density in order to correct the measured quality factor for the intrinsic losses of the cell. Besides differences in the sound velocity and density between the sample and the reference liquid, differences in the attenuation coefficient may slightly affect the intrinsic losses of the cell.²⁵ Appropriate corrections have therefore been made to consider differences in the α values accordingly.²⁵ These corrections did never exceed 1.5% of the α value.

At frequencies between 10 MHz and 4.6 GHz absolute measurements of α have been performed by transmitting pulse-modulated sonic waves through a cell of variable sample length.^{26–28} Five cells have been employed that mainly differ from one another by the piezoelectric transmitter and receiver units. For measurements below 180 MHz²⁷ two cells were available in which quartz transducer disks (fundamental frequency $\nu_T = 1 \text{ MHz}$, diameter $d_T = 60$ and 40 mm , respectively)

**Figure 1.** Bilogarithmic plot of the α/ν^2 data as a function of frequency ν for the 0.25 M aqueous TED solutions at 25 °C. The full curve represents the graph of a Debye relaxation spectrum added to the classical contribution, $R_D(\nu)/(c_s\nu) + B' = (2\pi A_D \tau_D / c_s) / (1 + \omega^2 \tau_D^2) + B'$. The dashed line represents B' .

were operated at odd overtones of ν_T . Between 30 and 530 MHz²⁶ lithium niobate disks ($\nu_T = 10 \text{ MHz}$, $d_T = 12 \text{ mm}$) were excited at their odd overtones $(2n + 1)\nu_T$. Between 0.5 and 2 GHz broad-band end face excitation²⁹ of LiNbO₃ rods ($d_T = 3 \text{ mm}$, length $l_T = 10 \text{ mm}$) was applied.²⁸ In the range 1.1–4.6 GHz we used a cell in which the transducers were again operated in modes of thickness vibration. The actual transducers were thin ZnO films ($d_T = 2 \text{ mm}$, $\nu_T = 1.3 \text{ GHz}$) sputtered onto delay rods made of sapphire.²⁸ At each measuring frequency the transfer function $T(x)$ of the cells has been determined by successively varying the sample length and measuring T at 400 x values. The transfer characteristics of the electronic apparatus have been routinely recorded in additional runs in which the specimen cell was replaced by a high-precision below-cutoff piston attenuator used as a calibrated reference.

In the complete frequency range the measuring frequency ν was known and kept constant with a negligible error throughout. The temperature of the sample was controlled to within $\pm 0.01 \text{ K}$. Temperature gradients and differences in the temperature of different cells did not exceed 0.05 K, corresponding to the small estimated error of less than 0.1% in the attenuation coefficient. The total uncertainty of the α values measured with the resonator method is mostly due to possible slight changes in the mechanical cell adjustment by the cleaning and refilling procedure when the sample is exchanged for the reference liquid. The α values derived from the variable path length pulse-modulated wave transmission measurements may be affected by an imperfect parallelism of the transmitter and receiver unit and by an insufficient correction for diffraction losses. Strictly, the experimental errors in the attenuation coefficient depend on the individual α values themselves. Globally, however, the accuracy of the α data may be characterized by the errors listed in Table 2.

Sound Velocity. Between 200 kHz and 15 MHz the sound velocity c_s of the samples has been determined from the frequencies of successive main cell resonance peaks, taking into account the nonequidistant distribution of the resonance frequencies.^{30,31} The error in these c_s data (Table 1) is smaller than 0.1%. At high frequencies additional c_s values were available from the waviness of the transfer function $T(x)$ due to multiple reflections at small transducer spacing x .

3. Results in Terms of a Relaxation Model

Characteristics of the Absorption Spectra. Within the frequency range of measurements the dispersion in the sound velocity c_s of the TED solutions is small: $(c_s(2 \text{ GHz}) - c_s(200 \text{ kHz}))/c_s(200 \text{ kHz}) < 0.003$. It is thus easily possible to switch between the different formats $\alpha(\nu)/\nu^2$, $\alpha(\nu)\lambda$, and $\alpha_{\text{exc}}(\nu)\lambda$ where sonic absorption coefficients are favorably displayed as a function of frequency ν . Here, $\lambda = c_s/\nu$ is the wavelength.

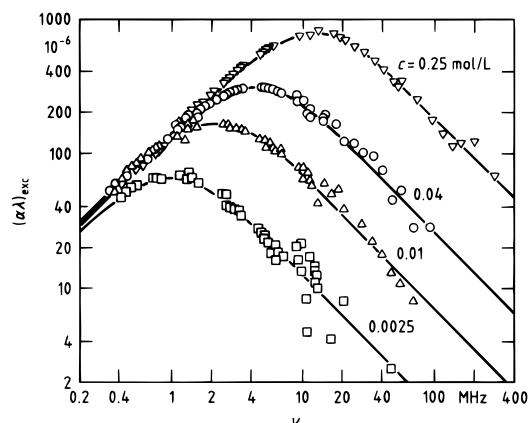


Figure 2. Excess absorption per wavelength at 25 °C displayed versus frequency for the aqueous TED solutions of low solute concentration c . The curves represent a Debye term (eq 2) with the parameter values found by a nonlinear least-squares regression analysis (Table 3).

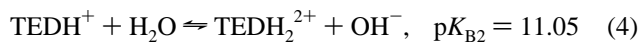
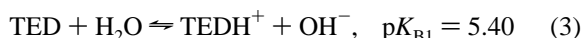
In Figure 1, the absorption coefficient α per ν^2 of the 0.25 M aqueous TED solution is displayed as a function of frequency. In the frequency range between about 1 and 100 MHz the α/ν^2 data clearly exhibit dispersion characteristics ($d(\alpha/\nu^2)/d\nu < 0$) and adopt the constant B' value at higher frequencies. Hence, there exists a frequency dependent contribution α_{exc} in excess of the classical part in the total absorption coefficient. It is found that in all solutions with TED concentration $c \leq 0.25$ mol/L (Figure 2) the excess absorption per wavelength can be well represented by a Debye-type relaxation spectral function³² R_D with discrete relaxation time τ_D :

$$R_D(\nu) = A_D \frac{\omega\tau_D}{1 + (\omega\tau_D)^2} \quad (2)$$

Here, $\omega = 2\pi\nu$ is the angular frequency and A_D is a relaxation amplitude.

As illustrated by Figure 3, two well-separated relaxation regions exist in the spectra of solutions with higher TED content ($c > 0.25$ mol/L). An analysis of these spectra reveals that the relaxation with a relaxation frequency $(2\pi\tau_D)^{-1}$ at a few MHz is again characterized by a discrete relaxation time. The additional excess absorption contributions at higher frequencies, however, extend over a broader frequency band than a Debye term, thus indicating that there exists a distribution of relaxation times.

Protolysis. At low solute concentration, protolysis of TED^{14,15} is governed by the following equilibrium constants:³³



Since, by definition,

$$K_{B1} = c(\text{TEDH}^+)c(\text{OH}^-)/c(\text{TED}) \quad (5)$$

$$K_{B2} = c(\text{TEDH}_2^{2+})c(\text{OH}^-)/c(\text{TEDH}^+) \quad (6)$$

and

$$c = c(\text{TED}) + c(\text{TEDH}^+) + c(\text{TEDH}_2^{2+}) \quad (7)$$

the concentration of the species involved in the coupled equilibria of eqs 3 and 4 can be calculated if the conservation of electrical charges is taken into account:

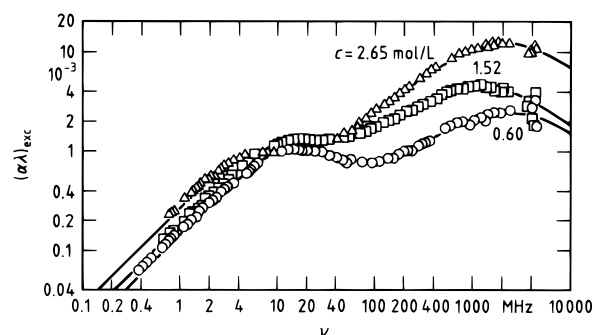


Figure 3. Excess absorption spectra at 25 °C plotted for aqueous TED solutions of higher solute concentration c . The curves are graphs of the model spectral function (eq 18) with the parameter values displayed in Table 3.

$$0 = c(\text{TEDH}^+) + 2c(\text{TEDH}_2^{2+}) + c(\text{H}_3\text{O}^+) - c(\text{OH}^-) + \theta \quad (8)$$

In eq 8 θ considers charges from additionally present ions as Na^+ in the sodium hydroxide solutions and Cl^- in the hydrogen chloride solutions. Let

$$\Pi = c(\text{OH}^-)c(\text{H}_3\text{O}^+) = 10^{-14} \text{ mol/L} \quad (9)$$

denote the ion product of water, then follows:

$$0 = c^4(\text{OH}^-) + (K_{B1} - \theta)c^3(\text{OH}^-) + K_{B1}(K_{B2} - c - \Pi/K_{B1} - \theta)c^2(\text{OH}^-) - K_{B1}(2K_{B2}c + \Pi + \theta K_{B2})c(\text{OH}^-) - K_{B1}K_{B2}\Pi \quad (10)$$

This relation can be solved numerically by using the Newton method. For aqueous solutions without HCl or NaOH added ($\theta = 0$) with $K_{B1} = 3.98 \times 10^{-6}$ mol/L $\gg K_{B2} = 8.91 \times 10^{-12}$ mol/L, it approximately follows that

$$c(\text{TEDH}^+) = c(\text{OH}^-) = K_{B1}((1 + 4c/K_{B1})^{1/2} - 1)/2 \quad (11)$$

and

$$c(\text{TEDH}_2^{2+}) = K_{B2} \quad (12)$$

and thus $c(\text{TEDH}_2^{2+}) < 10^{-7}c(\text{TEDH}^+)$. The second step (eq 4) in the coupled protolysis reactions can, therefore, be completely neglected in the spectra of the aqueous TED solutions ($\theta = 0$). For this reason the Debye-type relaxation (eq 2) is taken to represent the TEDH⁺/TED equilibrium (eq 3) of those systems.

If NaOH is added, the coupled equilibria (eqs 3 and 4) between the different TED species are, of course, even more shifted toward the left-hand side of eq 3. Hence, the above arguments for a Debye-type relaxation are again valid. In the acidic solutions the concentration of unprotonated TED molecules is so small that just the TEDH⁺/TEDH₂²⁺ reaction adds noticeable contributions to the sonic spectrum. Again, the excess absorption can be described by a discrete relaxation time (Figure 4).

Concentration Fluctuations. The above arguments indicate that the additional relaxation term in the spectra of the TED solutions of higher solute content (Figure 3) is not due to a protolysis reaction. The facts that this term is found at $c > 0.25$ mol/L only and that it is subject to a relaxation time distribution suggest this contribution to the sonic spectra to reflect fluctuations in the local TED concentration. We therefore

aimed at its description by a relevant theoretical model of concentration fluctuations, particularly by the unifying model that has been derived recently.³⁴ This unifying model combines aspects of previous theories of non-critical concentration fluctuations as well as theories of density fluctuations,^{11,20,35–41} and it has been found to enable a uniform description of a variety of binary aqueous solutions of different organic solute series.³⁴ It is interesting to call to mind that mixtures of amines with water show a clear tendency to phase separate at a critical demixing temperature. Triethylamine/water and 2,6-dimethylpyridine/water mixtures are prominent examples, the sonic spectra of which have been intensively studied previously^{42–46} and have been discussed in terms of critical fluctuation dynamics, particularly in the light of the Bhattacharjee–Ferrell dynamic scaling theory.^{47,48}

The unifying model of noncritical fluctuations is based on the assumption that changes in the local concentration and structure of the liquids are enabled by two mechanisms, namely by diffusion and, alternatively, by a process that is characterized by a discrete relaxation time τ_0 . Hence, the time dependence of the autocorrelation function

$$\phi(r,t) = \langle \chi(r,t)\chi(0,0) \rangle / \langle |\chi(0,0)|^2 \rangle \quad (13)$$

of a suitable order parameter χ is governed by the differential equation

$$\partial\phi(r,t)/\partial t = (D\nabla^2 - \tau_0^{-1})\phi(r,t) \quad (14)$$

This model also takes into account existing spatial correlation in the autocorrelation function so that, different from the original Romanov–Solov'ev theory,^{35,36} $\phi(r > 0, 0)$ needs not to be identical with zero. Different from the treatment of concentration fluctuations in ionic systems¹¹ where the long-ranging Coulombic interactions suggested an Ornstein–Zernike ansatz,^{49,50} a $\phi(r,0)$ function has been taken here, which indeed follows the Ornstein–Zernike behavior at large r values but decreases toward small r . Owing to this particular choice, the model relaxation spectral function $R_{\text{um}}(\nu)$ can be defined without introducing an artificial maximum wavenumber q_{max} , corresponding to a minimum interaction length l_{min} .^{11,35,36}

The spectral function of the unifying model can be expressed as

$$R_{\text{um}}(\nu) = Q \int_0^\infty \frac{q^2}{(1 + 0.164q\xi + 0.25(q\xi)^2)^2} \frac{\omega\tau_i}{1 + (\omega\tau_i)^2} dq \quad (15)$$

Herein Q is the amplitude factor of the Romanov–Solov'ev theory,^{35,36} ξ is the correlation length of the fluctuations in the order parameter, and τ_i is a characteristic time, which, according to the relation

$$\tau_i^{-1} = Dq^2 + \tau_0^{-1} \quad (16)$$

corresponds to the wavenumber q in the spectrum of fluctuations. Since the spatial correlation in the fluctuations at $r \geq \xi$ follows the Ornstein–Zernike ansatz $\phi(r,t) \approx \exp(-r/\xi)/r$, the Ferrell equation⁵¹

$$\xi = k_B T / (6\pi\eta_s D) \quad (17)$$

has been used here to relate ξ to the mutual diffusion coefficient D . In eq 17 k_B denotes the Boltzmann constant.

The Romanov–Solov'ev amplitude Q is a function of the second derivatives, with respect to the mole fraction of the

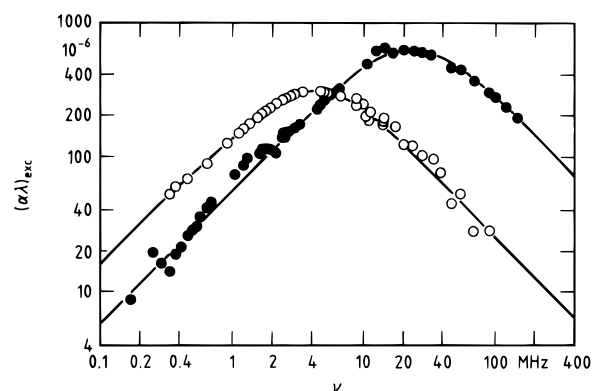


Figure 4. Ultrasonic excess absorption per wavelength at 25 °C plotted as a function of frequency for the 0.04 M aqueous TED solution with (●, $c_{\text{HCl}} = 0.08$ mol/L) and without (○) HCl added. The curves are graphs of a Debye relaxation term (eq 2) with the parameter values given in Table 3.

dispersed phase, of the Gibbs free energy, of the molar volume and of the molar enthalpy. Under favorable conditions, if these thermodynamic quantities are known with sufficient accuracy to allow for the calculation of their second differentials, the Q data obtained from the sonic spectra can be compared to those derived from the thermodynamic parameters,¹¹ or Q may be treated even as a known parameter in the evaluation of the ultrasonic attenuation spectra. For the TED solutions, since we do not know of sufficiently accurate data of the three thermodynamic quantities, Q is treated as an unknown parameter here.

Model Relaxation Spectral Function. Following the above lines of reasoning, the measured attenuation per wavelength spectra have been analytically described by the relaxation function

$$R(\nu) = R_D(\nu) + R_{\text{um}}(\nu) + B\nu \quad (18)$$

It turned out that the process with discrete relaxation time τ_0 is not required in order to adequately represent the spectra of the TED solutions. Hence, all spectra can be characterized by a maximum number of five parameters, namely, A_D , τ_D , Q , ξ , and B . The values of these parameters are displayed in Table 3. They have been obtained from a regression analysis by which, using the Marquardt algorithm,⁵² the reduced variance was minimized.

4. Discussion

Protonation of TED: First Step. The amplitude of a Debye relaxation term representing a stoichiometrically well-defined chemical reaction (eqs 3 and 4) is related to the isentropic molar volume change ΔV_s according to the relation⁵³

$$A_D = \frac{\pi c_s^2 \sigma \Gamma}{RT} (\Delta V_s)^2 \quad (19)$$

Herein, R is the gas constant and Γ is given by the concentrations $c(A_i)$ of the species A_i involved in the reaction under consideration,

$$\Gamma^{-1} = \sum_i c^{-1}(A_i) \quad (20)$$

The isentropic volume change according to

$$\Delta V_s = \Delta V_T - \frac{\alpha_p}{\rho c_p} \Delta H \quad (21)$$

is related to the isothermal volume change ΔV_T and the enthalpy

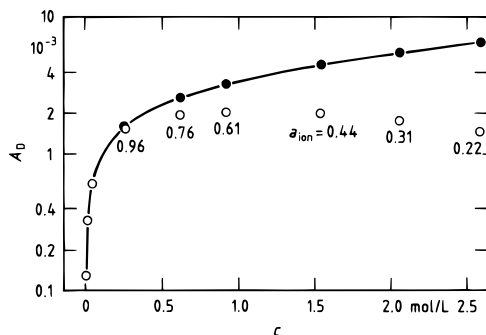


Figure 5. Amplitude of the Debye-type relaxation term in the model relaxation spectral function (eq 18) resulting from the measured spectra (O) and as calculated with the aid of eqs 19 and 20 assuming $\Delta V_S = 33.5 \text{ cm}^3/\text{mol}$ (full curve). The full points show the A_D values from the measured spectra when the activity coefficients a_{ion} are used in the evaluation of the data.

TABLE 3: Amplitude A_D and Relaxation Time τ_D of the Low-Frequency Debye Term R_D in the Model Relaxation Function $R(\nu)$ that Represents the Ultrasonic Absorption Spectra of the Aqueous TED System (Eq 18), Amplitude Parameter Q and Correlation Length ξ of the R_{um} Term in $R(\nu)$, as Well as the B Parameter that Characterizes the Extrapolated High-Frequency Behavior of the Absorption Per Wavelength (Eq 18)

$c, \text{mol/L}$	$A_D, 10^{-3}$ $\pm 2\%$	τ_D, ns $\pm 4\%$	$Q, 10^{-30} \text{m}^3$ $\pm 5\%$	$\xi, 10^{-10} \text{m}$ $\pm 5\%$	B, ps $\pm 0.5\%$
25 °C, Water, pH = 10.0–11.5					
0.0025	0.129	162			32.1
0.01	0.332	73.3			32.3
0.04	0.616	36.6			33.0
0.25	1.54	13.7			33.8
0.601	1.95	11.6	0.18	3.9	34.3
0.904	2.03	11.7	0.29	4.1	36.2
1.52	1.98	13.1	0.38	4.2	43.0
2.04	1.77	19.1	0.29	3.2	51.7
2.56	1.49	26.7	0.27	2.0	61.6
15 °C, Water					
0.01	0.279	110			43.6
35 °C, Water					
0.01	0.378	56.4			24.8
25 °C, 0.01 mol/L NaOH, pH = 12.0					
0.04	0.083	3.8			32.4
25 °C, 0.1 mol/L NaOH, pH = 13.0					
0.908			0.30	4.0	36.3
25 °C, 0.08 mol/L HCl, pH = 2.2					
0.04	1.28	6.7			32.0

change ΔH accompanied by the process. In eq 21 $a_p = V^{-1}(\partial V/\partial T)_p$ denotes the coefficient of thermal expansion and c_p is the specific heat at constant pressure p . Together with the concentration data obtained from eqs 7 and 11, relations 19 and 20 can be used to derive the isentropic volume change ΔV_S from the Debye term amplitudes A_D . For the solutions of low TED content ($c < 0.25 \text{ mol/L}$), $\Delta V_S = 33.5 \text{ cm}^3/\text{mol}$ follows at 25 °C. In view of $\Delta V_S = 26.9 \text{ cm}^3/\text{mol}$ for the dissociation/neutralization of water ($\Delta V_T = 23.5 \text{ cm}^3/\text{mol}$, $\Delta H = -13.7 \text{ kcal/mol}$ ⁵⁴), this appears to be a reasonable value. As shown by Figure 5 however, eq 19 does not apply for the solutions of higher TED concentration. There appears to be a discrepancy between the amplitudes $A_{D \text{ meas}}$ derived from the measured spectra (Table 3) and the amplitudes $A_{D \text{ calc}}$ calculated according to eqs 19 and 20. This discrepancy obviously increases with c . It is a reasonable assumption to relate the difference between the $A_{D \text{ meas}}$ and the $A_{D \text{ calc}}$ to an activity coefficient $a_{\text{ion}} \neq 1$ in the ion concentration. The values of this activity coefficient, which are required to adjust the amplitudes from eqs 19 and 20

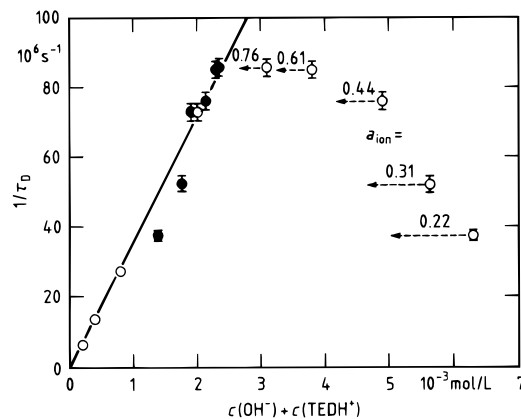


Figure 6. Relaxation rate τ_D^{-1} plotted versus the sum $c(\text{OH}^-) + c(\text{TEDH}^+)$ of anion and cation concentrations. Circles indicate the τ_D^{-1} data from the measured spectra. Full points refer to the same data after consideration of the activity coefficients a_{ion} .

so that $A_{D \text{ calc}} = A_{D \text{ meas}}$, are numerically given in Figure 5 and are graphically displayed in Figure 10.

Quite remarkably, the activity coefficients obtained from the relaxation amplitudes are also consistent with the relaxation time data τ_D (Table 3). The relaxation rate $1/\tau_D$ of the reaction step under consideration (eq 3) is expected to follow the relation¹⁹

$$\tau_D^{-1} = k_{B1}^r(c(\text{TEDH}^+) + c(\text{OH}^-)) + k_{B1}^f \quad (22)$$

where k_{B1}^r and k_{B1}^f denote the reverse (recombination) and the forward (dissociation) rate constants, respectively. As illustrated by Figure 6, at lower TED concentration ($c < 0.25 \text{ mol/L}$) the measured data again follow the theoretical predictions (eq 22) if the c values from eqs 7 and 11 are simply used as the active concentrations ($a_{\text{ion}} = 1$). At higher TED content the theoretical relations pretty well account for the measured relaxation rates if the c values in eq 22 are multiplied by the activity coefficients a_{ion} from Figure 5.

From the plot of $1/\tau_D$ as a function of $a_{\text{ion}}(c(\text{TEDH}^+) + c(\text{OH}^-))$ in Figure 6, $k_{B1}^r = (3.6 \pm 0.3) \times 10^{10} \text{ L}/(\text{mol s})$ is derived, a value that is characteristic of proton-transfer processes in aqueous solutions^{55,56} or, more generally, of reactions that are diffusion-controlled.¹⁹ The dissociation rate constant follows as $k_{B1}^f = K_{B1}/k_{B1}^r = (1.4 \pm 0.2) \times 10^5 \text{ s}^{-1}$. It is only briefly mentioned here that similar rate constants govern the protolysis of ammonia in water:⁵⁵ $k^r = 3.4 \times 10^{10} \text{ L}/(\text{mol s})$, $k^f = 6 \times 10^5 \text{ s}^{-1}$.

By application of eq 22, the rate constants obtained from the spectra of the simple TED solutions can be used to calculate the shift in the ultrasonic relaxation spectrum on changes of the pH of the solutions. As illustrated by Figure 7, the spectrum of a TED solution with NaOH added is quite reasonably predicted by the data derived from the measurements.

Following the Eyring formula⁵⁷

$$\tau_D = \frac{A_r}{T} \exp(-\Delta G^\ddagger/(RT)) \quad (23)$$

the activation Gibbs energy ΔG^\ddagger has been calculated from the temperature dependence in the relaxation time data. In eq 23, A_r denotes a factor. We found $\Delta G^\ddagger = -(5.7 \pm 0.7) \text{ kcal/mol}$, which corresponds to $\Delta G^\ddagger = -4.4 \text{ kcal/mol}$ for the protolysis of ammonia.⁵⁸

TEDH⁺/TEDH₂²⁺ Equilibrium. The addition of a sufficient amount of a strong acid (e.g., HCl; see Figure 4) leads to an increase in the TEDH₂²⁺ concentration so that the second step in the protolysis equilibrium (eq 4) dominates the first one (eq

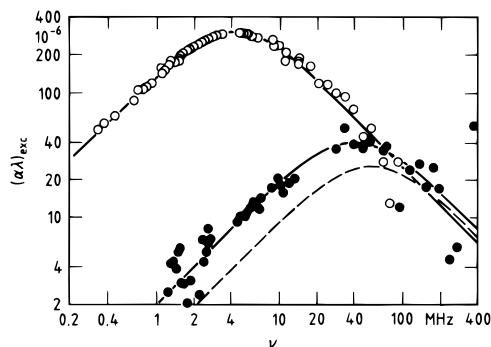


Figure 7. Ultrasonic excess absorption spectrum of a 0.04 M aqueous TED solution at 25 °C without (O) and with (●) NaOH (0.01 mol/L) added. The dashed curve shows the spectrum for the TED/NaOH/H₂O system as predicted from the ΔV_s , k_{B1}^f , and k_{B1}^r data of the aqueous TED systems.

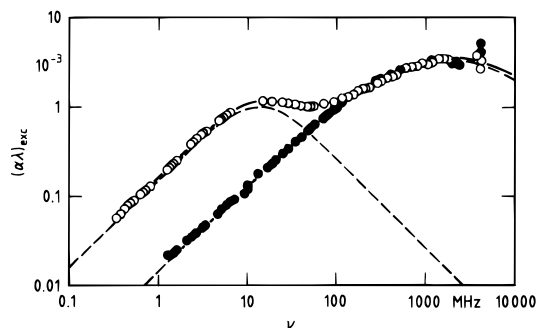


Figure 8. Ultrasonic excess absorption per wavelength, $(\alpha\lambda)_{exc}$, displayed as a function of frequency for a 0.9 M aqueous TED solution at 25 °C (O) and for the same solution with NaOH (●, 0.1 mol/L) added. The dashed curve indicates the subdivision of the spectrum of the former solution into a low-frequency Debye-type spectral term $R_D(\nu)$ and a term $R_{um}(\nu)$ due to concentration fluctuations (eq 18).

3) in the sonic relaxation spectrum. If eq 22 is rewritten to apply the second reaction step

$$\tau_D^{-1} = k_{S2}^r(c(\text{TEDH}^+) + c(\text{H}_3\text{O}^+)) + k_{S2}^f \quad (24)$$

the rate constants k_{S2}^r and k_{S2}^f of the reverse (recombination) and forward (dissociation) processes, respectively, can be derived from the relaxation rate data and the equilibrium constant K_{S2} , where $\text{p}K_{S2} = 14 - \text{p}K_{B2}$ (eq 4). The values $k_{S2}^r = 1.1 \times 10^{10}$ L/(mol s) and $k_{S2}^f = 1.3 \times 10^7$ s⁻¹ result. The finding of $k_{S2}^r \approx k_{B1}^r/3$ reflects the repulsive Coulombic force between the TEDH^+ ion and the additional proton, consistent with the arguments by Eigen et al.⁵⁵ The comparatively high value for the rate constant k_{S2}^f of the dissociation process indicates a rather small stability of the TEDH_2^{2+} complex in an acidic solvent.

An analogous application of eq 19 allows for the determination of the isentropic volume change, which turns out to be as small as 16.2 cm³/mol only. The significant difference to the (adiabatic) reaction volume of the first step of protonation is assumed to reflect a noticeable difference in the rearrangement of the hydration structure between both steps of protolysis. Charging of the neutral molecule, obviously, leads to substantially stronger changes in the hydration properties than addition of a further electrical charge to the already protonated TED.

TED Association. Our assumption of the high-frequency relaxation term in the spectra of aqueous TED solutions to be due to concentration fluctuations is substantiated by results for solutions with sodium hydroxide added. In Figure 8, the sonic excess absorption spectrum for 0.9 mol/L TED in water and also in a solution of 0.1 mol/L in H₂O is shown. From the

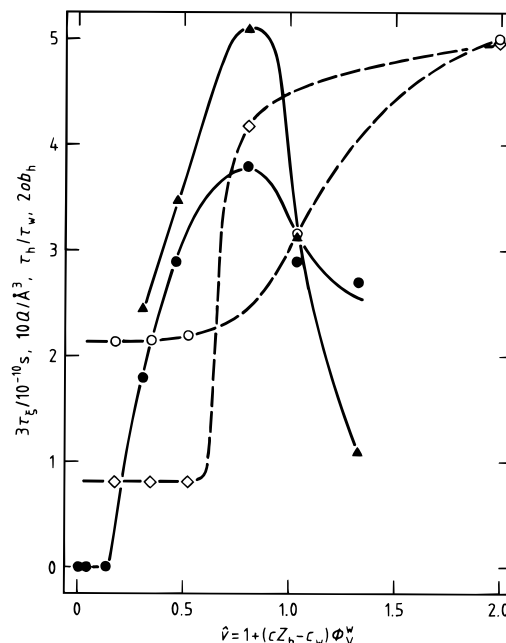


Figure 9. The characteristic decay time τ_ξ (▲) and amplitude parameter Q (●) of the $R_{um}(\nu)$ term in the model relaxation spectral function (eq 18), as well as the hydration water to pure water relaxation time ratio τ_h/τ_w (○) and the hydration water relaxation time distribution parameter b_h (◇) from dielectric spectra⁵⁹ for aqueous solutions of triethylenediamine plotted versus the volume fraction $\hat{\nu}$ of hydrated TED molecules (Z_h , number of hydration water molecules per TED molecules; c_w , molar concentration of water in the solutions; ϕ_w^v , molar volume of water at 25 °C).

rate constants derived from the aforementioned spectra for aqueous TED solutions, no noticeable relaxation term due to protolysis reactions is expected to exist in the systems with added NaOH. According to these expectations, the Debye-type relaxation in the lower frequency range is in fact absent in the TED/NaOH/water system (Figure 8). The high-frequency relaxation, however, which has been related to concentration fluctuations in the evaluation of the spectra, remains unaltered if water is exchanged for the aqueous NaOH solution. Obviously, this relaxation term does not noticeably depend on the extent of protonation of TED molecules.

The spectrum for the TED/NaOH/water system (Figure 8), where the contributions from the fluctuations in the TED concentration are not masked by an additional Debye relaxation term, may also be taken to clearly indicate the suitability of the unifying model. The small values found for the ξ parameter ($2 \text{ \AA} \leq \xi \leq 4.2 \text{ \AA}$; see Table 3) indicate that there do not exist long-ranging spatial correlations in the aqueous TED solutions. It is, however, worthy to note that application of the spectral function eq 15 to the Romanov–Solov'ev model yields $\xi \leq l_{min}$, where $l_{min} = 1 \text{ \AA}$ typically. Hence $\xi > 2 \text{ \AA}$ clearly shows that spatial correlations cannot be neglected in the TED/water systems.

In Figure 9, the Romanov–Solov'ev amplitude parameter Q and the characteristic time

$$\tau_\xi = \xi^2/(4D) = \frac{3\pi\eta_s\xi^3}{2k_B T} \quad (25)$$

that describes the decay by diffusion of fluctuations with typical length ξ are plotted as a function of the volume fraction $\hat{\nu}$ of hydrated TED molecules. The values for this $\hat{\nu}$ parameter have been obtained by discussing dielectric spectra of aqueous TED

solutions in terms of a hydration model⁵² assuming Z_h water molecules per molecule of solute to be affected in their dielectric properties.

Both Q and τ_ξ increase at $\hat{v} > 0.25$ to adopt a relative maximum in the range of \hat{v} values that correspond to the closest packing of hydrated TED molecules, which are assumed to be equally sized and spherically shaped. The ratio of the hydration water to pure water relaxation times, also derived from dielectric spectra,⁵⁹ increases in this range of \hat{v} values from $\tau_h/\tau_w = 2.15 \pm 0.1$ at $\hat{v} < 0.6$ ($v < 0.11$; v , volume fraction of TED) to much higher values. A relaxation time $\tau_h \approx 2 \tau_w$ is characteristic of many solutes.⁶⁰ The significant increase in τ_h when strong overlaps of the hydration region occur is assumed to reflect the reduced density of hydrogen bonding sites offered to a hydration water molecule to form a new bond.⁶⁰

Also in the range of \hat{v} values around that of the closest packing of spheres, the parameter b_h , which measures the width of the underlying hydration water relaxation time distribution, increases substantially, thus pointing to a change in the microdynamic behavior of the water surrounding TED molecules. We conclude that at small solute content ($\hat{v} \leq 0.15$, $c \leq 0.25$ mol/L) the TED molecules appear to be rather randomly distributed. At higher TED content concentration fluctuations exist as indicated by a nonvanishing amplitude parameter Q . As a result of hydrophobic effects, the TED molecules obviously tend to form associates that, as shown by the τ_ξ data, increase until the volume fraction of the hydrated solute molecules adopts a value around that of the closest packing of spheres. In that concentration region association of TED molecules leads to an increase in both the characteristic relaxation time and the width of the relaxation time distribution of the hydration water. Owing to the lack of excess water, a tendency toward a more monodisperse liquid structure results at even higher solute concentration, as visualized by the decreasing correlation decay time τ_ξ .

Volume Viscosity, Adiabatic Compressibility. According to the relation⁶¹

$$\eta_v = \frac{\rho c_s^2}{2\pi^2} B - \frac{4}{3} \eta_s \quad (26)$$

the volume viscosity η_v of the TED solutions can be globally related to the part Bv in the ultrasonic absorption per wavelength and to the shear viscosity η_s . By application of eq 26, small effects of energy dissipation from the sonic field due to heat conduction are neglected and the solutions are considered homogeneous liquids with respect to their high-frequency ultrasonic properties. The volume viscosity to shear viscosity ratios resulting from the B values of Table 3 by using eq 26 are displayed as a function of solute concentration in Figure 10. The rather high η_v/η_s ratio for water ($\eta_v/\eta_s = 2.7$, 25 °C) is assumed to be due to the open structure of the hydrogen-bonded liquid with a suggested structure relaxation frequency well above our frequency range of measurement.⁶¹ As usually found with aqueous solutions, the addition of the solute leads to a reduction in the η_v/η_s ratio. This reduction may be taken to reflect the disturbance of the hydrogen bond network and the partial breakdown of the voluminous water structure resulting thereby. Within this series of TED solutions, however, the viscosity ratio does not reach the limiting value $\eta_v/\eta_s = 0.67$ (dashed line in Figure 10), which is assumed to apply for liquids without a structural relaxation at very high frequencies.^{62,63}

The successive breakdown of the hydrogen network structure of the solvent water by adding of TED is also reflected by the compressibility data displayed in Figure 10. The adiabatic compressibility

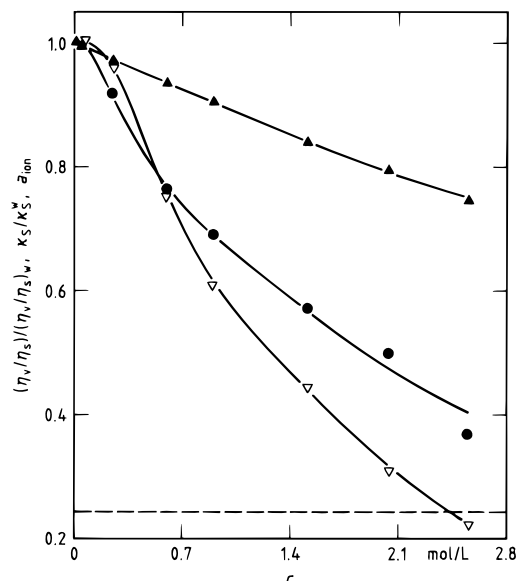


Figure 10. Relative volume to shear viscosity ratio $(\eta_v/\eta_s)(\eta_v/\eta_s)_w^{-1}$ (●), normalized adiabatic compressibility κ_s/κ_s^w , and activity coefficient a_{ion} (▽) of aqueous TED solutions at 25 °C displayed as a function of solute concentration c . The dashed curve indicates the viscosity ratio $\eta_v/\eta_s = 2/3$. w denotes pure water data.

$$\kappa_s = \rho^{-1} c_s^{-2} \quad (27)$$

of the solutions has been calculated from the sound velocity data measured at around 1 MHz (Table 1). Again, owing to its open structure, water is characterized by a rather high compressibility ($\kappa_s = 4.479 \times 10^{-10} \text{ m}^2 \text{ N}^{-1}$, 25 °C). It decreases with increasing TED concentration. Hence, both global quantities, η_v and κ_s , do not show a special behavior at the solute content that corresponds to the volume fraction of the closest packing of (spherically shaped) hydrated TED molecules.

5. Conclusions

Ultrasonic spectra of solutions of triethylenediamine in water and also in aqueous sodium hydroxide are capable of showing contributions from two different elementary relaxation mechanisms. The chemical relaxation with a relaxation frequency around 10 MHz reflects either step in the protolysis reactions of the weak base, $\text{TED} + \text{H}_2\text{O} \rightleftharpoons \text{TEDH}^+ + \text{OH}^-$ at high pH and the step $\text{TEDH}_2^{2+} + \text{H}_2\text{O} \rightleftharpoons \text{TEDH}^+ + \text{H}_3\text{O}^+$ at low pH. An evaluation of the chemical relaxation term allows the forward and reverse rate constants and the isentropic volume change of the reactions to be determined and also the activity coefficients of the first step of protolysis to be presented as a function of the solute concentration. The relaxation with a relaxation frequency around 1 GHz is subject to a relaxation time distribution. It exists at higher TED concentrations only and can be favorably represented by an extended model of the Romanov–Solov'ev theory of concentration fluctuations. Hence, consistent with results from dielectric spectrometry, we have to conclude that the TED molecules form associates in aqueous solutions with solute concentration $c > 0.5$ mol/L. This association appears to be largely independent of the pH. Obviously, it is due to hydrophobic effects. This is a rather unexpected result, since normally molecules with n -alkane groups rather tend to associate, while TED is an almost compact globularly shaped molecule.

Acknowledgment. Financial support by the Deutsche Forschungsgemeinschaft is gratefully acknowledged.

References and Notes

- (1) Franks, F., Ed. *Water, A Comprehensive Treatise*; Plenum: New York, 1972–1982; Vols. 1–7.
- (2) Tanford, C. *The Hydrophobic Effect: Formation of Micelles and Biological Membranes*; Wiley Interscience: New York, 1980.
- (3) Ben-Naim, A. *Hydrophobic Interactions*; Plenum: New York, 1980.
- (4) Stillinger, F. H. *Science* **1980**, *209*, 4455.
- (5) Pratt, L. R. *Annu. Rev. Phys. Chem.* **1985**, *36*, 433.
- (6) Franks, F., Ed. *Water Science Reviews*; Cambridge University Press: Cambridge, 1985–1989; Vols. 1–4.
- (7) Jancso, G.; Cser, L.; Grosz, T.; Ostanevich, Y. M. *Pure Appl. Chem.* **1994**, *66*, 515.
- (8) Brai, M.; Kaatze, U. *J. Phys. Chem.* **1992**, *96*, 8946.
- (9) Rupprecht, A. Diploma Thesis: Georg-August-Universität, Göttingen, Germany, 1994.
- (10) Gailus, T. Dissertation, Georg-August-Universität, Göttingen, Germany, 1996.
- (11) Kühnel, V.; Kaatze, U. *J. Phys. Chem.* **1996**, *100*, 19747.
- (12) Menzel, K.; Rupprecht, A.; Kaatze, U. *J. Phys. Chem.* **1997**, *101*, 1255.
- (13) Pottel, R.; Kaatze, U. *Ber. Bunsen-Ges. Phys. Chem.* **1969**, *73*, 437.
- (14) Wen, W.-Y.; Takeguchi, N.; Wilson, D. P. *J. Solution Chem.* **1974**, *3*, 103.
- (15) Hsieh, Y. C.; Inglefield, P. T.; Wen, W.-Y. *J. Solution Chem.* **1974**, *3*, 351.
- (16) Kaatze, U.; Wen, W.-Y. *J. Phys. Chem.* **1978**, *82*, 109.
- (17) Pörschke, D.; Eggers, F. *Eur. J. Biochem.* **1972**, *26*, 490.
- (18) Slutsky, L. J. In *Methods of Experimental Physics*; Edmonds, P. D., Ed.; Academic: New York, 1981; Vol. 19, p 179.
- (19) Strehlow, H. *Rapid Reactions in Solutions*; VCH Verlagsgesellschaft: Weinheim, 1992.
- (20) Romanov, V. P.; Ul'yanov, S. V. *Physica* **1993** *A201*, 527.
- (21) Ferrell, R. A.; Bhattacharjee, J. K. *Phys. Rev.* **1985** *A31*, 1788.
- (22) Kaatze, U.; Trachimow, C.; Pottel, R.; Brai, M. *Ann. Phys. (Leipzig)* **1996**, *5*, 13.
- (23) Eggers, F.; Kaatze, U.; Richmann, K. H.; Telgmann, T. *Meas. Sci. Technol.* **1994**, *5*, 1131.
- (24) Kaatze, U.; Wehrmann, B.; Pottel, R. *J. Phys. E: Sci. Instrum.* **1987**, *20*, 1025.
- (25) Kononenko, V. S. *Sov. Phys. Acoust.* **1985**, *31*, 499.
- (26) Kaatze, U.; Lautscham, K.; Brai, M. *J. Phys. E: Sci. Instrum.* **1988**, *21*, 98.
- (27) Kaatze, U.; Kühnel, V.; Menzel, K.; Schwerdtfeger, S. *Meas. Sci. Technol.* **1993**, *4*, 1257.
- (28) Kaatze, U.; Kühnel, V.; Weiss, G. *Ultrasonics* **1996**, *34*, 51.
- (29) Bömmel, H. E.; Dransfeld, K. *Phys. Rev. Lett.* **1958**, *1*, 234.
- (30) Labhardt, A. M.; Schwarz, G. *Ber. Bunsen-Ges. Phys. Chem.* **1976**, *80*, 83.
- (31) Eggers, F.; Kaatze, U. *Meas. Sci. Technol.* **1996**, *7*, 1.
- (32) Debye, P. *Polare Molekeln*; Hirzel: Leipzig, 1929.
- (33) Larson, J. W.; Bertrand, G. L.; Hepler, L. G. *J. Chem. Eng. Data* **1966**, *11*, 595.
- (34) Rupprecht, A. Dissertation, Georg-August-Universität, Göttingen, Germany, 1997.
- (35) Romanov, V. P.; Solov'ev, V. A. *Sov. Phys. Acoust.* **1965**, *11*, 68.
- (36) Romanov, V. P.; Solov'ev, V. A. *Sov. Phys. Acoust.* **1965**, *11*, 219.
- (37) Isakovich, M. A.; Chaban, I. A. *Sov. Phys. JETP* **1966**, *23*, 893.
- (38) Solov'ev, V. A.; Montrose, C. J.; Watkins, M. H.; Litovitz, T. A. *J. Chem. Phys.* **1968**, *48*, 2155.
- (39) Montrose, C. J.; Litovitz, T. A. *J. Acoust. Soc. Am.* **1970**, *47*, 1250.
- (40) Romanov, V. P.; Solov'ev, V. A. In *Water in Biological Systems*; Vuks, M. F., Sidrova, A. J., Eds.; Consultant Bureaus: New York, 1971; Vol. 2, p 1.
- (41) Endo, H. *J. Chem. Phys.* **1990**, *92*, 1986.
- (42) Yun, S. S. *J. Chem. Phys.* **1970**, *52*, 5200.
- (43) Gutschick, V. P.; Pings, C. J. *J. Chem. Phys.* **1971**, *55*, 3845.
- (44) Garland, C. W.; Lai, C. N. *J. Chem. Phys.* **1978**, *69*, 1342.
- (45) Fast, S. J.; Yun, S. S. *J. Chem. Phys.* **1985**, *83*, 5888.
- (46) Kaatze, U.; Schreiber, U. *Chem. Phys. Lett.* **1988**, *148*, 241.
- (47) Bhattacharjee, J. K.; Ferrell, R. A. *Phys. Rev. A* **1981**, *24*, 1643.
- (48) Ferrell, R. A.; Bhattacharjee, J. K. *Phys. Rev. A* **1985**, *31*, 1788.
- (49) Ornstein, L. S.; Zernike, F. *Phys. Z.* **1918**, *19*, 134.
- (50) Ornstein, L. S.; Zernike, F. *Phys. Z.* **1926**, *27*, 762.
- (51) Ferrell, R. A. *Phys. Rev. Lett.* **1970**, *24*, 1169.
- (52) Marquardt, D. W. *J. Soc. Ind. Appl. Math.* **1963**, *2*, 2.
- (53) Faber, H.; Petrucci, S. In *The Chemical Physics of Solvations*; Dogonadze, R. R., et al., Eds.; Elsevier: Amsterdam, 1986; Part B.
- (54) Eigen, M.; De Maeyer, L. *Z. Elektrochem.* **1955**, *59*, 986.
- (55) Eigen, M.; Kruse, W.; Maass, G.; De Maeyer, L. In *Progress in Reaction Kinetics*; Porter, G., Jennings, K. R., Stevens, B., Eds; Pergamon Press: Oxford, 1964; Vol. 2, p 286.
- (56) Eigen, M. In *Fast Reactions and Primary Processes in Chemical Kinetics*; Claesson, S., Ed.; Nobel Symposium 5; Almqvist & Wiksell: Stockholm, 1968; p 245.
- (57) Eyring, H.; Powell, *Adv. Colloid Sci.* **1941**, *1*, 183.
- (58) Frost, A. A.; Pearson, R. G. *Kinetics and Mechanisms*; Wiley: New York, 1961.
- (59) Kaatze, U.; Pottel, R. *J. Mol. Liq.* **1985**, *30*, 115.
- (60) Kaatze, U. *Radiat. Phys. Chem.* **1995**, *45*, 549.
- (61) Davis, C. M.; Jarzynski, J. In *Water, a Comprehensive Treatise*; Franks, F., Ed.; Plenum: New York, 1972; Vol. 1, p 443.
- (62) Madigosky, W. M.; Warfield, R. W. *J. Chem. Phys.* **1983**, *78*, 1912.
- (63) Madigosky, W. M.; Warfield, R. W. *Acustica* **1984**, *55*, 123.